

UC Davis

UC Davis Previously Published Works

Title

Clonidine inhibits anti-non-Gal IgM xenoantibody elicited in multiple pig-to-primate models

Permalink

<https://escholarship.org/uc/item/6015p9xr>

Journal

Xenotransplantation, 22(6)

ISSN

0908-665X

Authors

Stewart, John M
Tarantal, Alice F
Hawthorne, Wayne J
[et al.](#)

Publication Date

2015-11-01

DOI

10.1111/xen.12199

Peer reviewed



Published in final edited form as:

Xenotransplantation. 2015 ; 22(6): 413–426. doi:10.1111/xen.12199.

Clonidine inhibits anti-non-Gal IgM xenoantibody elicited in multiple pig-to-primate models

John M. Stewart¹, Alice F. Tarantal², Wayne J. Hawthorne^{3,4}, Evelyn J. Salvaris⁵, Philip J. O’Connell^{3,4}, Mark B. Nottle⁶, Anthony J. F. d’Apice^{5,7}, Peter J. Cowan^{5,7}, and Mary Kearns-Jonker¹

¹Department of Human Anatomy, Loma Linda University School of Medicine, Loma Linda, CA

²Departments of Pediatrics and Cell Biology and Human Anatomy, and California National Primate Research Center, University of California, Davis, CA, USA

³Centre for Transplant and Renal Research, Westmead Millennium Institute, Westmead, NSW

⁴National Pancreas Transplant Unit, University of Sydney at Westmead Hospital, Westmead, NSW

⁵Immunology Research Centre, St. Vincent’s Hospital Melbourne, Melbourne, Vic

⁶Discipline of Obstetrics and Gynaecology, University of Adelaide, Adelaide, SA

⁷Department of Medicine, University of Melbourne, Melbourne, Vic., Australia

Abstract

Background—Survival of vascularized xenografts is dependent on pre-emptive inhibition of the xenoantibody response against galactosyltransferase knockout (GTKO) porcine organs. Our analysis in multiple GTKO pig-to-primate models of xenotransplantation has demonstrated that the anti-non-gal- α -1,3-gal (anti-non-Gal) xenoanti-body response displays limited structural diversity. This allowed our group to identify an experimental compound which selectively inhibited induced anti-non-Gal IgM xenoantibodies. However, because this compound had an unknown safety profile, we extended this line of research to include screening small molecules with known safety profiles allowing rapid advancement to large animal models.

Methods—The NIH clinical collections of small molecules were screened by ELISA for their ability to inhibit xenoantibody binding to GTKO pig endothelial cells. Serum collected from non-immunosuppressed rhesus monkeys at day 14 post-injection with GTKO pig endothelial cells was utilized as a source of elicited xenoantibody for initial screening. Virtual small molecule screening based on xenoanti-body structure was used to assess the likelihood that the identified small molecules bound xenoantibody directly. As a proxy for selectivity, ELISAs against tetanus toxoid and the natural antigens laminin, thyroglobulin, and single-stranded DNA (ssDNA) were utilized to assess the ability of the identified reagents to inhibit additional antibody responses. The identified inhibitory small molecules were further tested for their ability to inhibit xenoantibody elicited in multiple settings, including rhesus monkeys pre-treated with an anti-non-Gal selective

anti-idiotypic antibody, non-immunosuppressed rhesus monkeys immunized with wild-type fetal pig isletlike cell clusters, and non-immunosuppressed baboons transplanted with GTKO multiple transgenic pig kidneys.

Results—Four clinically relevant small molecules inhibited anti-non-Gal IgM binding to GTKO pig endothelial cells in vitro. Three of these drugs displayed a limited region of structural similarity suggesting they may inhibit xenoantibody by a similar mechanism. One of these, the anti-hypertensive agent clonidine, displayed only minimal inhibition of antibodies elicited by vaccination against tetanus toxoid or pre-existing natural antibodies against laminin, thyroglobulin, or ssDNA. Furthermore, clonidine inhibited elicited anti-non-Gal IgM from all animals that demonstrated a xenoantibody response in each experimental setting.

Conclusions—Clinically relevant small molecule drugs with known safety profiles can inhibit xenoantibody elicited against non-Gal antigens in diverse experimental xenotransplantation settings. These molecules are ready to be tested in large animal models. However, it will first be necessary to optimize the timing and dosing required to inhibit xenoantibodies in vivo.

Keywords

baboon; clonidine; endothelial cell; islet; kidney; pig; rhesus monkey; small molecule; xenotransplantation

Introduction

Xenotransplantation of genetically modified porcine organs and cells is approaching clinical relevance [1]. Multiple laboratories have demonstrated xenoislet survival of over 1 yr using non-human primate recipients [2–4], and transplantation of encapsulated pig pancreatic islets is currently in clinical trials [5]. More critically, in the extremely onerous vascularized heart transplant model, Mohiuddin et al. [6] achieved a median survival time of over 200 days with a maximum survival time of approximately 600 days at the time of publication [reported in supplementary discussion in print edition], albeit in a non-life supporting pig-to-primate model. Pre-emptively inhibiting the xenoantibody response against non- α -1,3-gal terminal disaccharide (non-Gal) antigens present on pig xenografts is important for long-term survival of vascularized xenografts [6–8] and thus translation to the clinic. To this end, perioperative B-cell depletion with anti-CD20 dramatically prolongs survival of cardiac xenografts [8]. However, in the context of transplantation, B-cell depletion is known to result in a greater risk of infection and infection-related death [9–11]. Targeted inhibition of the anti-non-Gal humoral immune response both perioperatively and long-term postoperatively could enhance xenograft survival while preserving the greater portion of B-cell-mediated adaptive immunity to ward off infection.

Our group has previously demonstrated that the elicited anti-non-Gal xenoantibody response displays limited structural diversity in multiple galactosyltransferase knockout (GTKO) pig-to-primate models of xenotransplantation [12,13]. This enabled us to identify an anti-non-Gal selective anti-idiotypic single-chain antibody and an experimental small molecule capable of selectively inhibiting induced anti-non-Gal IgM xenoantibodies [14]. Although in vitro this small molecule could inhibit the binding of residual IgM xenoantibody in animals

pre-treated with anti-idiotypic antibody, it had an unknown safety profile. We therefore extended this line of research to include screening of the NIH clinical collections, which consist almost entirely of small molecules with a history of use in clinical trials. We report here the identification of small molecule drugs with known safety profiles which selectively inhibit anti-non-Gal xenoantibody, allowing rapid translation to experiments in large animal models.

Materials and methods

Animals

Fifteen juvenile and two adult rhesus monkeys (*Macaca mulatta*) from the California National Primate Research Center, University of California, Davis, CA, were utilized in this study. All procedures met the requirements of the Animal Welfare Act. Protocols were approved prior to implementation by the University of California, Davis Institutional Animal Care and Use Committee.

Six baboons (*Papio hamadryas*) were supplied by the NH&MRC Australian National Baboon Colony, Sydney, Australia. All procedures were approved by Local Area Health Service Animal Ethics Committees and conducted in compliance with State Government legislation and NH&MRC Animal Research Guidelines.

Models of xenotransplantation

Immunization with GTKO pig aortic endothelial cells—Fifteen juvenile rhesus monkeys were screened for low levels of non-Gal-reactive xenoantibody by ELISA as previously reported [14]. Five animals with the lowest levels of pre-existing anti-non-Gal IgM xenoantibody were selected for further study. Two non-immunosuppressed animals (NIS.A and NIS.B) were intravenously injected with GTKO pig aortic endothelial cells (PAECs) in the absence of immunosuppression. This allowed for the induction of an anti-nonGal xenoantibody response without the procedural complications of islet or solid-organ xenotransplantation. Three additional animals (AIA.A-C) were pre-treated with a novel anti-non-Gal selective anti-idiotypic single-chain antibody (B4N190). This anti-idiotypic antibody was generated in our laboratory using a sequence-and structure-based approach to select a reagent specific for induced anti-non-Gal antibody. The anti-idiotypic antibody was administered once per week for 3 weeks before immunization with GTKO PAECs.

Islet xenotransplantation—Two non-immunosuppressed adult rhesus monkeys (ISLET. 1-2) were immunized with wild-type fetal porcine isletlike cell clusters to elicit a xenoantibody response, as previously reported [15]. Briefly, fetal porcine isletlike cell clusters (15×10^6 cells) were prepared by culturing collagenase-digested pancreata from fetuses at 66 days of gestation (term = ~114 days). Cells were cultured for 1 to 3 weeks before intraperitoneal injection on experimental day 0. Serum samples from the current set of studies were collected before immunization on day 0 and on day 8 after immunization.

Kidney xenotransplantation—Genetically modified pigs (*Sus scrofa*), which were GTKO and co-expressed human CD55, CD59, and α 1,2-fucosyltransferase (H-transferase,

HT), were generated by Cowan et al. [16,17]. Six non-immunosuppressed baboons (KIDNEY.1-6) were transplanted with GTKO/hCD55/hCD59/hHT pig kidneys. Additional details regarding the conditions of transplant will be published separately by our collaborators. The grafts from two animals (KIDNEY.1 and KIDNEY.2) survived over 100 h. This was a sufficient length of time for the anti-non-Gal xenoantibody response to be detectable in peripheral blood. Serum samples from the current studies were collected from these two animals on day 0 and at the time of rejection.

Small molecule library

The NIH Clinical Collections 1 and 2 composed of 446 and 281 compounds, respectively, consist of drugs selected for their history of use in clinical trials, purity, solubility, and availability from commercial sources. The NIH Clinical Collections were provided through the National Institutes of Health Molecular Libraries Roadmap Initiative. Fifty microliters of each drug was provided in a 96-well plate format diluted to 10 mM in DMSO. Further, these drugs were dispensed into 96-well plates in an anoxic environment and stored at -70°C to ensure minimal degradation during shipping and storage before screening.

In vitro small molecule screening

The xenoantibody response and inhibition by small molecule drugs were measured by ELISA as previously described [18] but using GTKO/hCD55 PAECs as targets. GTKO/hCD55 PAECs (NSRRC:0009) were purchased from the National Swine Research and Resource Center (Columbia, MO, USA). Initial screening for drugs with the ability to inhibit xenoantibody responses was performed to identify promising candidates. These candidates were then tested in triplicate with at least two independent repeated experiments. Individual plates of drugs were allowed to thaw at room temperature before drugs were diluted to $60\ \mu\text{M}$ in blocking solution for screening. Blocking solution was composed of $1\times$ phosphate-buffered saline (pH 7.4) with 0.05% Tween-20 and 2% bovine serum albumin. This was then mixed 1 + 1 with serum (1 : 50 in blocking solution) to obtain a solution with a final drug concentration of $30\ \mu\text{M}$ and serum 1 : 100 dilution. This solution was allowed to equilibrate at room temperature for 15 to 30 min before incubation with GTKO/hCD55 PAECs at room temperature for 1 h. Anti-human IgM HRP (1 : 1000) (Jackson Immunoresearch, West Grove, PA, USA) was used as a secondary antibody. Each plate of NIH Clinical Collection drugs was re-frozen at -70°C after each study and utilized a maximum of five times. After initial screening, each drug identified to inhibit anti-non-Gal IgM xenoantibody was purchased from a commercial source.

In silico small molecule screening

The anti-non-Gal IgM xenoantibody response is known to display a high degree of sequence variation in the heavy- and light-chain third complementarity determining regions (CDRs) [12,13]. Thus, inclusion of multiple xenoantibody structural models was required to refine our previous virtual screening process and account for this inherent structural variation. All three xenoantibody models were encoded by representative xenoantibody sequences, which were highly similar within the CDR1 and CDR2 regions. Consistent with our previous analysis, each heavy chain utilized the IGHV3-66 and IGHJ4 germline genes. However, the heavy-chain CDR3 amino acid translation displayed a high degree of variation. All three

xenoantibody models utilized in our refined small molecule screening protocol were generated using the ROSIE antibody-modeling server [19], which has been demonstrated to have comparable accuracy to discovery studio [20] which we previously utilized. The combination of AutoDock Vina [21] and PyRx [22] were used to perform virtual screening over the entire antigen-binding region of each model. The entirety of the NIH clinical collections was screened against each xenoantibody model. The results of each independent screen were ranked by predicted affinity. Those molecules from the NIH clinical collection which were predicted to be in the top 30% using all three xenoantibody structural models, and inhibited xenoantibody in vitro, were considered to be the most likely to bind directly to anti-non-Gal xenoantibody.

Natural antibody ELISA

Natural antibody ELISAs were performed as previously described [14]. Briefly, single-stranded DNA (ssDNA) (Sigma, St. Louis, MO, USA), laminin (Sigma), and thyroglobulin (Sigma) were pre-coated on 96 96-well plates at a concentration of 20 $\mu\text{g}/\text{well}$. Serum (1 : 100) with or without drug (30 μM) in blocking solution was incubated 1 h at room temperature with the antigen of interest. Anti-human IgM HRP (1 : 1000) (Jackson Immunoresearch) was used as a secondary antibody. After 10-min incubation at room temperature with 100 μl of OPD solution (Pierce Biotechnology, Rockford, IL, USA), development was stopped using 50 μl of 2.5 M sulfuric acid and read at 490 nm.

Tetanus toxoid IgG ELISA

Tetanus toxoid IgG titer ELISA was performed according to the manufacturer's instructions (Genway biotech, San Diego, CA, USA) with one exception. Either a stock small molecule suspension or an equal volume of vehicle was added as necessary to the serum diluent of the experimental and control conditions, respectively. Serum was diluted 1 : 101 as per the manufacturer's instructions while the final concentration of clonidine was 30 μM . A standard curve calibrated against the World Health Organization reference preparation enabled us to quantify anti-tetanus toxoid IgG in international units per milliliter (IU/ml).

Statistical analysis

All statistical analyses were performed using Excel. Data are represented as mean \pm standard error of the mean (SEM) of at least three technical replicates. Statistical significance (P-value <0.05) was established using a two-tailed Student's *t*-test or analysis of variance as appropriate.

Results

Screening for clinically relevant small molecule drugs capable of inhibiting anti-non-Gal xenoantibody

Serum collected from non-immunosuppressed animals 14 days after injection with GTKO PAECs was used as a source of anti-non-Gal IgM xenoantibody for screening. Drugs were initially screened for the ability to inhibit induced xenoantibodies from one monkey (NIS.A) because this animal had a larger anti-non-Gal xenoantibody response allowing more sensitive detection of inhibition. This also minimized the quantity of serum required in

early-stage screening experiments. However, promising candidates were retested for the ability to inhibit binding of xenoantibodies elicited in both NIS.A and NIS.B. Over the course of screening all 727 molecules, four compounds were identified to inhibit 23 to 64% of IgM xenoantibody elicited in non-immunosuppressed rhesus monkeys (Fig. 1). Gabexate mesilate, a protease inhibitor utilized in treatment of acute pancreatitis [23], was able to inhibit 24 to 34% of induced IgM xenoantibody. Oxiconazole, an azole anti-fungal agent [24], was able to inhibit 31 to 48% of induced IgM xenoantibody. Clonidine, an α_2 adrenergic receptor agonist most commonly used to treat hypertension [25], was able to inhibit 30 to 48% of induced IgM xenoantibody. Voriconazole, a triazole anti-fungal agent [24], was able to inhibit 39 to 64% of induced IgM xenoantibody.

In silico small molecule screening suggests azole anti-fungals bind directly to xenoantibody

All xenoantibody sequences utilized in antibody modeling were representative of those elicited in baboons responding to xenotransplantation with GTKO/hCD55/hCD59/hHT neonatal isletlike cell clusters [13]. We sought to refine our previous in silico screening process by more accurately representing the diversity of xenoantibody CDR3 regions. The ROSIE antibody-modeling server [19] was utilized to generate three xenoantibody models. Variations in xenoantibody CDR3 amino acid sequences resulted in notable differences in the predicted structure of the heavy-chain CDR3 and to a lesser degree the light-chain CDR3 (Fig. 2). However, these differences had little impact on the structures and relative positioning of the heavy- and light-chain CDR1 and CDR2 loops.

Neither gabexate mesilate nor clonidine was included in the list of molecules predicted to bind xenoantibody. However, four structurally related azole anti-fungal agents were predicted to bind all three xenoantibody structural models with high affinity including ketoconazole, voriconazole, clotrimazole, and oxiconazole. Given that both voriconazole and oxiconazole were identified to inhibit xenoantibody by screening in vitro, we were prompted to retest all azole anti-fungals included in the NIH clinical collection. Unfortunately, no additional xenoantibody inhibitors were identified. Interestingly, both oxiconazole and voriconazole are the most structurally similar pair of these four drugs. Furthermore, they share a limited region of structural similarity with clonidine (Fig. 3), suggesting all three molecules may share a similar mechanism of inhibition. Of note, both voriconazole and oxiconazole likely bind directly to anti-non-Gal xenoantibody given that they were both predicted in silico and identified in vitro. However, oxiconazole is only suitable for topical use and thus would not be appropriate for application as a xenoantibody inhibitor in vivo. Thus, further experiments did not include oxiconazole.

Natural IgM antibodies are minimally affected by clonidine and moderately affected by gabexate mesilate and voriconazole

In order to determine whether the identified compounds could inhibit other antibody responses, we tested their ability to interfere with natural IgM antibodies. Serum collected at day 14 after injection of NIS.A and NIS.B with GTKO PAECs was used as a source of antibody. This was essential because the identified compounds were known to inhibit IgM xenoantibody present at this time point. Ideally, these compounds would not interact with

natural antibodies which would suggest a high level of selectivity for anti-non-Gal xenoantibodies. Gabexate mesilate and voriconazole displayed a moderate level of selectivity while clonidine demonstrated a high level of selectivity for anti-non-Gal IgM xenoantibody (Fig. 4). Gabexate mesilate and voriconazole displayed minimal interference of binding to laminin (Fig 4A,B); however, both inhibited a proportion of natural antibodies that bound to thyroglobulin (16 to 38%; Fig. 4C,D) and ssDNA (13 to 50%; Fig. 4E,F). In contrast, clonidine inhibited a relatively small proportion of anti-ssDNA antibody binding in only one animal ($19 \pm 1\%$ in NIS.B; Fig. 4E,F) and had no significant effect on other types of natural antibodies examined. Therefore, in this context, clonidine displayed the highest level of selectivity for anti-non-Gal IgM xenoantibody.

Clinically relevant small molecule drugs can provide added benefit in vitro in combination with anti-idiotypic antibody in vivo

While these drugs can inhibit xenoantibody when utilized in isolation, it is more likely that they will be used in combination with other immunosuppressive reagents in vivo. We sought to test whether they could provide additional benefit in the context of pre-treatment with an anti-non-Gal selective anti-idiotypic antibody. Three rhesus monkeys (AIA.A-C) were pre-treated with anti-idiotypic antibody intravenously on experimental days -28, -21, and -14 before intravenous injections with GTKO PAECs on experimental day 0 (Fig. 5A). Serum collected from these animals on experimental day +14 was utilized as a source of induced xenoantibody for this experiment. Clonidine was able to reduce anti-non-Gal IgM detectable in serum samples from all animals tested (Fig. 5B). For one animal (AIA.A), the combination of clonidine and gabexate mesilate inhibited anti-non-Gal IgM to a greater extent than either drug alone. Additionally, the combination of gabexate mesilate and voriconazole inhibited detection of anti-non-Gal IgM binding in serum samples from two of three animals (AIA.A and AIA.B). It should be noted that the levels of anti-non-Gal IgM detected after combination treatment [anti-idiotypic antibody + small molecule(s)] were comparable to, or lower than that of the matched naïve animal (Fig. 5C) with only one exception (AIA.A + gabexate mesilate).

Anti-idiotypic antibody and clonidine have marginal impact on natural antibodies

Because it was effective in all animals tested, further experimentation in the context of pre-treatment with anti-idiotypic antibody utilized clonidine alone or in combination with gabexate mesilate. In order to investigate the impact of anti-idiotypic antibody and small molecule drugs on other antibody responses, we tested their ability to interfere with natural IgM antibodies (Fig. 6). Three animals were tested for the impact on natural antibodies against laminin, thyroglobulin, and ssDNA. Of the nine possible combinations [animals \times (natural antibody)], only two demonstrated a significant change. AIA.B demonstrated a $32 \pm 2\%$ reduction of anti-laminin antibody levels (Fig. 6A,B) but no change in anti-thyroglobulin antibodies (Fig. 6C,D) while AIA.A demonstrated a $32 \pm 1\%$ reduction of anti-ssDNA antibodies (Fig. 6E,F). Thus, pretreatment with the anti-idiotypic antibody was associated with only marginal changes in natural antibody levels. In this context, clonidine displayed minimal inhibition of the natural antibodies present at experimental day 14 (Fig. 6). Clonidine by itself displayed only marginal inhibition (10 to 21%) of natural anti-laminin IgM antibodies in two of three animals but did not impact any other classes of natural

antibodies (Fig. 6A, B). This suggests clonidine is highly selective for anti-non-Gal IgM xenoantibody. In contrast, gabexate mesilate, alone or in combination with clonidine, inhibited natural antibodies against laminin, thyroglobulin, and ssDNA. Gabexate mesilate inhibited anti-laminin antibodies from each animal (28 to 70%), anti-ssDNA antibodies from two animals (AIA.A and AIA.C; 45 to 56%), and anti-thyroglobulin antibodies from one animal (AIA.A; 42%). Thus, gabexate mesilate appears to have little specificity for anti-non-Gal IgM xenoantibody in this context.

Clonidine inhibits anti-non-Gal IgM xenoantibody elicited in rhesus monkeys after transplantation with fetal pig isletlike cell clusters

Clonidine was further tested for the ability to inhibit IgM xenoantibody elicited in rhesus monkeys in response to transplantation with fetal pig islet-like cell clusters. Two adult rhesus monkeys were transplanted with porcine isletlike cell clusters isolated from wild-type fetal pigs at day 66 of gestation [15]. Although we have studied the anti-gal carbohydrate antibody response of these animals, they also demonstrated a notable anti-non-Gal IgM xenoantibody response (Fig. 7). Serum collected at day 8 after xenotransplantation was used as a source of elicited anti-non-Gal xenoantibodies. As determined by ELISA, clonidine was able to inhibit over 50% of the anti-non-Gal IgM xenoantibodies elicited in both monkeys.

Clonidine selectively inhibits anti-non-Gal IgM xenoantibody elicited in baboons after GTKO pig kidney transplantation

IgM xenoantibodies elicited by kidney xenotransplantation in the absence of additional immunosuppression were measured with or without the addition of clonidine in vitro. Circulating anti-non-Gal xenoantibody is known to be dramatically reduced by absorption onto the graft in the first few days after transplant [26]. Thus, there were only detectable xenoantibody responses in two of the six baboons whose GTKO multiple transgenic kidney xenografts survived over 100 h (KID-NEY.1 and KIDNEY.2; Fig. 8A,B). Serum samples utilized in this study were collected just before transplant and at the time of rejection. As determined by ELISA, clonidine was able to inhibit $28 \pm 2\%$ and $75 \pm 1\%$ of the elicited anti-non-Gal IgM xenoantibody response of these two animals (Fig. 8A,B).

All six baboons were previously immunized and routinely boosted every 5 yr for tetanus. This allowed us to determine the impact of clonidine on the levels of a clinically relevant set of protective antibodies elicited by vaccination. Anti-tetanus toxoid IgG antibodies were unaffected by clonidine in five of six animals (Fig. 8C). In the other animal (KIDNEY.1), clonidine significantly reduced the detectable anti-tetanus toxoid IgG in post-transplant serum by 0.084 IU/ml. However, the remaining antibody (0.19 IU/ml) was still well above 0.10 IU/ml which is known to provide substantial protection against tetanus [27,28]. Furthermore, because clonidine was able to inhibit an equal or greater percentage of anti-non-Gal xenoantibodies from both animals that demonstrated a xenoanti-body response, we considered this outcome to show a high degree of selectivity in this experimental setting.

Discussion

In this study, we identified three clinically relevant small molecule drugs with the ability to selectively inhibit anti-non-Gal IgM xenoantibody. Clonidine maintained this capability when utilized against xenoantibodies elicited against pig endothelial cells as well as islet and kidney xenografts. Furthermore, clonidine was effective against elicited xenoantibody from all animals that demonstrated a xenoantibody response, including baboons and rhesus monkeys. Given that clonidine is consistently effective in such diverse experimental models of xenotransplantation, it is a highly promising candidate for in vivo studies.

The small molecule drugs identified in our current study may also have beneficial effects beyond selective inhibition of anti-non-Gal xenoantibody. For instance, clonidine has been used clinically in multiple settings for decades [25,29–35] and has well documented effects on the immune system. It has recently been found to prevent neutrophil extravasation by stabilizing endothelial cell expression of adherens junctional molecules [36]. Clonidine can also reduce serum concentrations of inflammatory cytokines such as IL-1 β and IL-6 in healthy young adults [37] and mitigate the postoperative rise of serum TNF- α in response to lower extremity revascularization [38]. Furthermore, voriconazole can be an effective anti-fungal prophylactic treatment [39] while gabexate mesilate's anticoagulant effect has been demonstrated to improve islet engraftment in a syngeneic rat model of islet transplantation [40]. Xenoislet engraftment could therefore be enhanced by inhibition of the instant blood-mediated inflammatory reaction as well as by inhibition of anti-non-Gal xenoantibody.

In our previous work, we identified an experimental small molecule, JMS022, from the NCI Diversity Set III that was capable of inhibiting xenoantibody elicited by GTKO PAECs [14]. While this library was large enough and sufficiently structurally diverse to enhance the likelihood of successful in silico screening, it was composed of small molecules with unknown safety profiles. The NIH Clinical Collections were selected for the current study because they consist almost entirely of drugs that have been in phase I to III clinical trials. Additionally, all compounds are available commercially. These two qualities dramatically enhanced the likelihood that any small molecule inhibitors of anti-non-Gal xenoantibody could be advanced rapidly and tested in vivo for efficacy in large animals. Furthermore, screening all 727 drugs in vitro ensured that we would not miss compounds that may not come up in virtual screening.

It is of particular interest that clonidine was able to effectively inhibit post-transplant/immunization xenoantibody from all animals that demonstrated a xenoantibody response. Furthermore, clonidine was effective against anti-non-Gal IgM xenoantibody elicited by endothelial cells, isletlike cell clusters, and kidney xenotransplantation. This is consistent with our previous analysis suggesting that the majority of the anti-non-Gal IgM antibody response is structurally restricted in multiple settings [12,13]. However, the previously identified experimental compound JMS022 was only capable of inhibiting the IgM xenoantibody response of three of five rhesus monkeys tested (NIS.A, AIA.A, and AIA.C) [14]. This suggested some degree of structural variation at the site to which JMS022 binds. We speculate that this may be due to previously noted variation in the structures of the CDR3 loops of the antibody heavy and light chains [13].

Our refined in silico screening methodology incorporates the structural variation of the CDR3 loops. Using this modified algorithm, oxiconazole and voriconazole, but not clonidine or gabexate, were both predicted to bind anti-non-Gal IgM xenoantibody with high affinity. This suggests that voriconazole and oxiconazole were capable of inhibiting xenoantibody directly. However, clonidine shares a limited region of structural similarity suggesting all three molecules may inhibit xenoantibody via a common mechanism. A recent analysis of 227 antigen-antibody complexes suggests that tyrosine and tryptophan residues in the hypervariable region almost exclusively interact with the corresponding target antigen [41]. Furthermore, these side chains are generally responsible for a large proportion of the binding free energy. Thus, hypervariable region tyrosine and tryptophan residues which are conserved in all three xenoantibody structural models (i.e., W32 in the light-chain CDR1, Y32, and Y33 in the heavy-chain CDR1, and Y50, Y58, and Y59 in the heavy-chain CDR2; [13]) are highly likely to mediate both xenoantibody–xenoantigen interactions and interact with small molecule inhibitors. The region of limited structural similarity shared between clonidine, voriconazole, and oxiconazole is likely to interact with these side chains via pi–pi interactions and halogen bonding. Unfortunately, neither of these mechanisms are accurately represented by the most accessible virtual screening or molecular docking programs as these programs utilize atomic point-charge-based calculations [42–45]. Therefore, further refinement is necessary to enable us to use computational modeling to more accurately predict which molecules will selectively inhibit xenoantibody.

In the current work, we utilized inhibition of natural antibodies against laminin, thyroglobulin, and ssDNA as a proxy for the ability of small molecule drugs to interfere with non-xenoantibody responses. The source of natural antibodies in primates is controversial [46,47]. However, natural antibodies are thought to contribute not only to immune pathologies [48] but also to normal physiologic processes [49] including immune surveillance [50]. Gabexate mesilate and voriconazole reduced natural antibody binding in the majority of animals tested, whereas clonidine did not. This suggests clonidine is a highly selective inhibitor of anti-non-Gal IgM xenoantibody.

Interference with the anti-tetanus antibody response elicited by vaccination represents a more clinically relevant measure of the ability of small molecules to affect non-xenoantibody responses. Clonidine only inhibited this protective induced category of antibodies in one of six animals tested. Furthermore, the detectable anti-tetanus toxoid IgG in this animal remained significantly above the lower limits of what is known to be protective in spite of inhibition by clonidine. Importantly, clonidine still displayed greater inhibition of anti-non-Gal IgM xenoantibody. Thus, clonidine displayed clinically relevant selectivity for anti-non-Gal xenoantibody while demonstrating efficacy in all animals that elicited a xenoantibody response.

It should be emphasized that no treatment in isolation, neither anti-idiotypic antibody nor small molecule, was capable of fully inhibiting the anti-non-Gal IgM xenoantibody response in all animals. It was only when both reagents were utilized in combination that the xenoantibody detected at experimental day 14 was comparable to or below those levels found in the naïve animals. Thus, these small molecule inhibitors of anti-non-Gal antibody

are likely to be the most effective when utilized in combination or in the context of additional reagents.

We have demonstrated that clonidine is effective in a diversity of settings and can inhibit anti-non-Gal xenoantibodies elicited not only by kidney or fetal isletlike cell cluster xenotransplantation, but also by pig endothelial cells. Together, these results indicate that it is feasible to block the initial anti-non-Gal IgM response in a targeted fashion, and also that the elicited xenoantibody responses are structurally related. Further scientific inquiry in these models should be focused in vivo. However, selective inhibitors are likely to be beneficial in these and related settings. For instance, selective inhibitors may be able to supplement or replace B-cell depletion which is currently required to extend GTKO cardiac xenotransplantation [6,8]. Recent advancements in genetic engineering have led to the generation of pigs with modifications that further reduce xenoantigen expression, including simultaneous inactivation of the GGTA1, CMAH, and β 4GalNT2 genes as reported by Estrada et al. [51]. As the dominant immunogen remaining on the cell surface of genetically modified pigs is altered, further studies will be needed to determine the impact of these changes on the functional efficacy of small molecule inhibitors. Thus, reagents capable of inhibiting anti-non-Gal xenoantibodies in a targeted fashion are a fruitful area of inquiry, and have the potential to enhance survival and/or function in multiple xenotransplantation settings.

Acknowledgments

This work was supported by NIH grant #RO1AI052079 (MKJ) and the California National Primate Research Center base operating grant #OD011107 (AFT).

Abbreviations

GTKO	galactosyltransferase knockout
PAEC	pig aortic endothelial cell
CDR	complementarity determining region
SEM	standard error of the mean

References

1. Cooper DK, Satyananda V, Ekser B, et al. Progress in pig-to-non-human primate transplantation models (1998–2013): a comprehensive review of the literature. *Xenotransplantation*. 2014; 21:397–419. [PubMed: 25176336]
2. Rogers SA, Chen F, Talcott MR, et al. Long-term engraftment following transplantation of pig pancreatic primordia into non-immunosuppressed diabetic rhesus macaques. *Xenotransplantation*. 2007; 14:591–602. [PubMed: 17991147]
3. van der Windt DJ, Bottino R, Casu A, et al. Long-term controlled normoglycemia in diabetic non-human primates after transplantation with hCD46 transgenic porcine islets. *Am J Transplant*. 2009; 9:2716–2726. [PubMed: 19845582]
4. Bottino R, Wijkstrom M, van der Windt DJ, et al. Pig-to-monkey islet xenotransplantation using multi-transgenic pigs. *Am J Transplant*. 2014; 14:2275–2287. [PubMed: 25220221]

5. Matsumoto S, Tan P, Baker J, et al. Clinical porcine islet xenotransplantation under comprehensive regulation. *Transplant Proc.* 2014; 46:1992–1995. [PubMed: 25131091]
6. Mohiuddin MM, Singh AK, Corcoran PC, et al. Genetically engineered pigs and target-specific immunomodulation provide significant graft survival and hope for clinical cardiac xenotransplantation. *J Thorac Cardiovasc Surg.* 2014; 148:1106–1113. discussion 1113–1104. [PubMed: 24998698]
7. Mohiuddin MM, Singh AK, Corcoran PC, et al. Role of anti-CD40 antibody-mediated costimulation blockade on non-Gal antibody production and heterotopic cardiac xenograft survival in a GTKO.hCD46Tg pig-to-baboon model. *Xenotransplantation.* 2014; 21:35–45. [PubMed: 24164510]
8. Mohiuddin MM, Corcoran PC, Singh AK, et al. B-cell depletion extends the survival of GTKO.hCD46Tg pig heart xenografts in baboons for up to 8 months. *Am J Transplant.* 2012; 12:763–771. [PubMed: 22070772]
9. Kamar N, Milioto O, Puissant-Lubrano B, et al. Incidence and predictive factors for infectious disease after rituximab therapy in kidney-transplant patients. *Am J Transplant.* 2010; 10:89–98. [PubMed: 19656128]
10. Petropoulou AD, Porcher R, Peffault De Latour R, et al. Increased infection rate after preemptive rituximab treatment for Epstein-Barr virus reactivation after allogeneic hematopoietic stem-cell transplantation. *Transplantation.* 2012; 94:879–883. [PubMed: 23001354]
11. Kelesidis T, Daikos G, Boumpas D, Tsiodras S. Does rituximab increase the incidence of infectious complications? A narrative review. *Int J Infect Dis.* 2011; 15:e2–e16. [PubMed: 21074471]
12. Kiernan K, Harnden I, Gunthart M, et al. The anti-non-gal xenoantibody response to xenoantigens on gal knockout pig cells is encoded by a restricted number of germline progenitors. *Am J Transplant.* 2008; 8:1829–1839. [PubMed: 18671678]
13. Chen Y, Stewart JM, Gunthart M, et al. Xenoantibody response to porcine islet cell transplantation using GTKO, CD55, CD59, and fucosyltransferase multiple transgenic donors. *Xenotransplantation.* 2014; 21:244–253. [PubMed: 24645827]
14. Stewart JM, Tarantal AF, Chen Y, et al. Anti-non-Gal-specific combination treatment with an anti-idiotypic Ab and an inhibitory small molecule mitigates the xenoanti-body response. *Xenotransplantation.* 2014; 21:254–266. [PubMed: 24635144]
15. Kleihauer A, Gregory CR, Borie DC, et al. Identification of the VH genes encoding xenoantibodies in non-immunosuppressed rhesus monkeys. *Immunology.* 2005; 116:89–102. [PubMed: 16108821]
16. Cowan PJ, Aminian A, Barlow H, et al. Renal xenografts from triple-transgenic pigs are not hyperacutely rejected but cause coagulopathy in non-immunosuppressed baboons. *Transplantation.* 2000; 69:2504–2515. [PubMed: 10910270]
17. Nottle MB, Beebe LF, Harrison SJ, et al. Production of homozygous alpha-1,3-galactosyltransferase knockout pigs by breeding and somatic cell nuclear transfer. *Xenotransplantation.* 2007; 14:339–344. [PubMed: 17669176]
18. Kearns-Jonker M, Fischer-Lougheed J, Shulkin I, et al. Use of lentiviral vectors to induce long-term tolerance to gal(+) heart grafts. *Transplantation.* 2004; 77:1748–1754. [PubMed: 15201677]
19. Lyskov S, Chou F-C, Conchúir SÓ, et al. Serverification of molecular modeling applications: the Rosetta Online Server that Includes Everyone (ROSIE). *PLoS ONE.* 2013; 8:e63906. [PubMed: 23717507]
20. Almagro JC, Beavers MP, Hernandez-Guzman F, et al. Antibody modeling assessment. *Proteins: Struct, Funct, Bioinf.* 2011; 79:3050–3066.
21. Trott O, Olson AJ. AutoDock Vina: improving the speed and accuracy of docking with a new scoring function, efficient optimization, and multithreading. *J Comput Chem.* 2010; 31:455–461. [PubMed: 19499576]
22. Wolf LK. New software and Websites for the chemical enterprise. *Chem Eng News.* 2009; 87:31.
23. Takeda K, Takada T, Kawarada Y, et al. JPN guidelines for the management of acute pancreatitis: medical management of acute pancreatitis. *J Hepatobiliary Pancreat Surg.* 2006; 13:42–47. [PubMed: 16463210]

24. Svecova L, Vrzal R, Burysek L, et al. Azole antimycotics differentially affect rifampicin-induced pregnane X receptor-mediated CYP3A4 gene expression. *Drug Metab Dispos.* 2008; 36:339–348. [PubMed: 17998298]
25. Viera AJ. Resistant hypertension. *J Am Board Fam Med.* 2012; 25:487–495. [PubMed: 22773717]
26. Le Bas-Bernardet S, Tillou X, Poirier N, et al. Xenotransplantation of galactosyl-transferase knockout, CD55, CD59, CD39, and fucosyl-transferase transgenic pig kidneys into baboons. *Transplant Proc.* 2011; 43:3426–3430. [PubMed: 22099813]
27. Crone NE, Reder AT. Severe tetanus in immunized patients with high anti-tetanus titers. *Neurology.* 1992; 42:761–764. [PubMed: 1565228]
28. Perry AL, Hayes AJ, Cox HA, Alcock F, Parker AR. Comparison of five commercial anti-tetanus toxoid immunoglobulin G enzyme-linked immunosorbent assays. *Clin Vaccine Immunol.* 2009; 16:1837–1839. [PubMed: 19793897]
29. Gourlay SG, Stead LF, Benowitz N. Clonidine for smoking cessation. *Cochrane Database Syst Rev.* 2004; 3:CD000058. [PubMed: 15266422]
30. Chan AK, Cheung CW, Chong YK. Alpha-2 agonists in acute pain management. *Expert Opin Pharmacother.* 2010; 11:2849–2868. [PubMed: 20707597]
31. Sigmon SC, Bisaga A, Nunes EV, et al. Opioid detoxification and naltrexone induction strategies: recommendations for clinical practice. *Am J Drug Alcohol Abuse.* 2012; 38:187–199. [PubMed: 22404717]
32. Cahill K, Stevens S, Perera R, Lancaster T. Pharmacological interventions for smoking cessation: an overview and network meta-analysis. *Cochrane Database Syst Rev.* 2013; (5):CD009329. [PubMed: 23728690]
33. Carroll I, Hah J, Mackey S, et al. Perioperative interventions to reduce chronic postsurgical pain. *J Reconstr Microsurg.* 2013; 29:213–222. [PubMed: 23463498]
34. Sallee F, Connor DF, Newcorn JH. A review of the rationale and clinical utilization of alpha2-adrenoceptor agonists for the treatment of attention-deficit/hyperactivity and related disorders. *J Child Adolesc Psychopharmacol.* 2013; 23:308–319. [PubMed: 23782125]
35. Freedman RR. Menopausal hot flashes: mechanisms, endocrinology, treatment. *J Steroid Biochem Mol Biol.* 2014; 142:115–120. [PubMed: 24012626]
36. Herrera-Garcia AM, Dominguez-Luis MJ, Arce-Franco M, et al. Prevention of neutrophil extravasation by alpha2-adrenoceptor-mediated endothelial stabilization. *J Immunol.* 2014; 193:3023–3035. [PubMed: 25114107]
37. Gourdin M, Dubois P, Mullier F, et al. The effect of clonidine, an alpha-2 adrenergic receptor agonist, on inflammatory response and posts ischemic endothelium function during early reperfusion in healthy volunteers. *J Cardiovasc Pharmacol.* 2012; 60:553–560. [PubMed: 22987052]
38. Nader ND, Ignatowski TA, Kurek CJ, Knight PR, Spengler RN. Clonidine suppresses plasma and cerebrospinal fluid concentrations of TNF-alpha during the perioperative period. *Anesth Analg.* 2001; 93:363–369. 363rd contents page. [PubMed: 11473862]
39. Karthaus M. Prophylaxis and treatment of invasive aspergillosis with voriconazole, posaconazole and caspofungin: review of the literature. *Eur J Med Res.* 2011; 16:145–152. [PubMed: 21486728]
40. Tokodai K, Goto M, Inagaki A, Imura T, Satomi S. Effect of synthetic protease inhibitor gabexate mesilate on attenuation of coagulant activity and cytokine release in a rat model of islet transplantation. *Transplant Proc.* 2011; 43:3176–3178. [PubMed: 22099749]
41. Robin G, Sato Y, Desplancq D, et al. Restricted diversity of antigen binding residues of antibodies revealed by computational alanine scanning of 227 antibody-antigen complexes. *J Mol Biol.* 2014; 26:3729–3743. [PubMed: 25174334]
42. Jorgensen WL, Schyman P. Treatment of halogen bonding in the OPLS-AA force field; application to potent anti-HIV agents. *J Chem Theory Comput.* 2012; 8:3895–3901. [PubMed: 23329896]
43. Liu Y, Xu Z, Yang Z, Chen K, Zhu W. A knowledge-based halogen bonding scoring function for predicting protein-ligand interactions. *J Mol Model.* 2013; 19:5015–5030. [PubMed: 24072554]
44. Ponder JW, Case DA. Force fields for protein simulations. *Adv Protein Chem.* 2003; 66:27–85. [PubMed: 14631816]

45. Oostenbrink C, Villa A, Mark AE, van Gunsteren WF. A biomolecular force field based on the free enthalpy of hydration and solvation: the GROMOS force-field parameter sets 53A5 and 53A6. *J Comput Chem.* 2004; 25:1656–1676. [PubMed: 15264259]
46. Griffin DO, Holodick NE, Rothstein TL. Human B1 cells in umbilical cord and adult peripheral blood express the novel phenotype CD20+ CD27+ CD43+ CD70. *J Exp Med.* 2011; 208:67–80. [PubMed: 21220451]
47. Covens K, Verbinnen B, Geukens N, et al. Characterization of proposed human B-1 cells reveals pre-plasmablast phenotype. *Blood.* 2013; 121:5176–5183. [PubMed: 23613519]
48. Boes M, Schmidt T, Linkemann K, et al. Accelerated development of IgG autoantibodies and autoimmune disease in the absence of secreted IgM. *Proc Natl Acad Sci U S A.* 2000; 97:1184–1189. [PubMed: 10655505]
49. Baumgarth N. The double life of a B-1 cell: self-reactivity selects for protective effector functions. *Nat Rev Immunol.* 2011; 11:34–46. [PubMed: 21151033]
50. Baumgarth N, Herman OC, Jager GC, et al. B-1 and B-2 cell-derived immunoglobulin M antibodies are nonredundant components of the protective response to influenza virus infection. *J Exp Med.* 2000; 192:271–280. [PubMed: 10899913]
51. Estrada JL, Martens G, Li P, et al. Evaluation of human and non-human primate antibody binding to pig cells lacking GGTA1/CMAH/ β 4GalNT2 genes. *Xenotransplantation.* 2015; 22:194–202. [PubMed: 25728481]

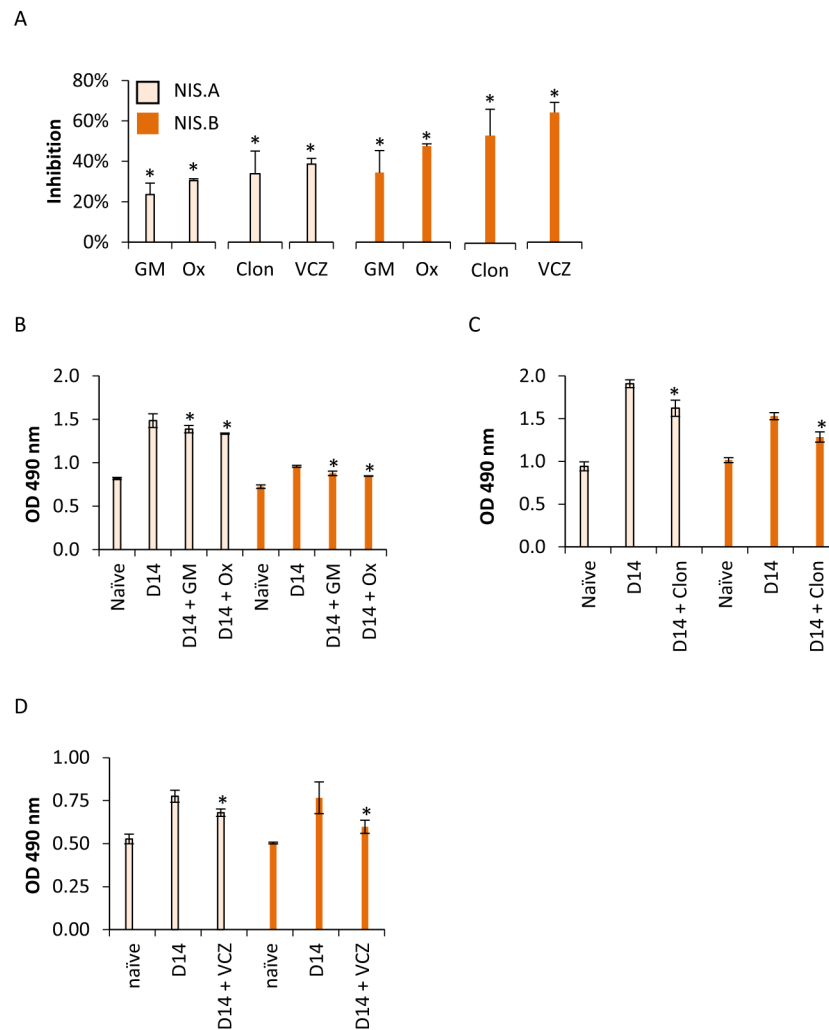


Fig. 1. The NIH clinical collections of small molecule drugs were screened by ELISA against galactosyltransferase knockout (GTKO)/hCD55 pig aortic endothelial cells. Serum collected from two non-immunosuppressed rhesus monkeys (NIS.A and NIS.B) at day 14 (D14) after immunization with GTKO pig endothelial cells was utilized as a source of elicited xenoantibody. Gabexate mesilate (GM), oxiconazole (OX), clonidine (Clon), and voriconazole (VCZ) were identified to inhibit elicited anti-non-Gal IgM. These drugs were able to inhibit 23.5 to 38.6% of the anti-non-Gal IgM xenoantibody elicited by NIS.A and 34.4 to 64.1% elicited by NIS.B. Values are reported as both the (A) % inhibition \pm the standard error of the mean (SEM) and (B–D) the optical density (OD) \pm SEM. % inhibition = $100\% \times [D14_{OD} - (D14 \text{ with drug})_{OD}] / (D14_{OD} - D0_{OD})$; *Indicates $P < 0.05$ compared to D14 without drug.

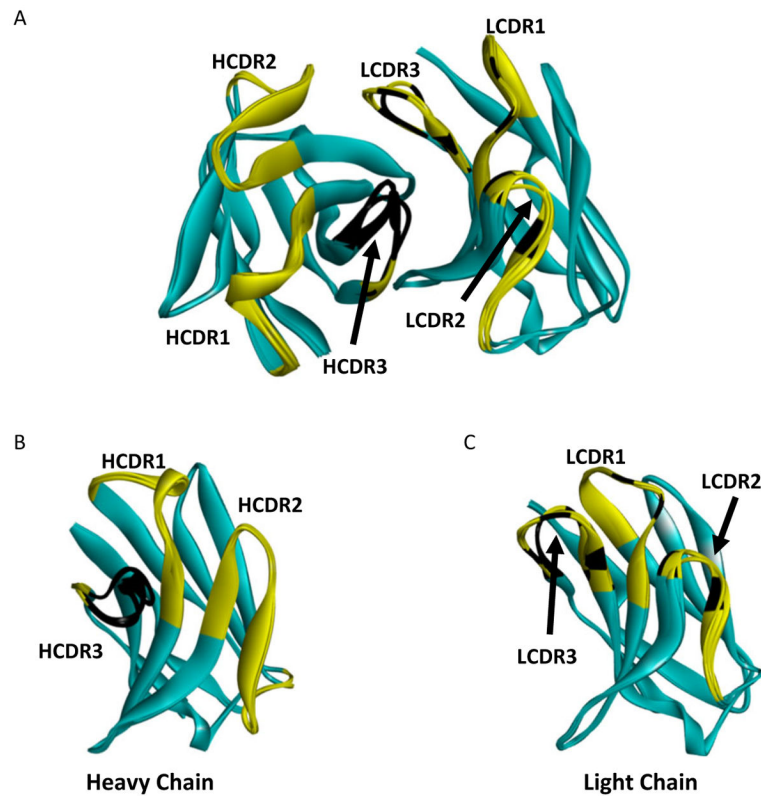


Fig. 2.

Three structural models of xenobody encoded by the germline genes IGHV3-66 and IGKV1D-12 are aligned. All xenobody sequences utilized for antibody modeling were derived from sequences elicited in baboons against galactosyltransferase knockout (GTKO)/hCD55/hCD59/hHT neonatal isletlike cell cluster transplantation [13]. (A) Computer modeling predicts that structure of the heavy-chain complementarity determining region (CDR) 3 displays a greater degree of structural variation than the light-chain CDR3. In contrast, the structures of the CDR loops 1 and 2 of both the (B) heavy- and (C) light-chain display minimal variation. CDR loops are highlighted in yellow for emphasis. Yellow—homologous region of complementarity determining region (CDR); black—non-homologous region of CDR; teal—framework regions; HCDR—heavy-chain CDR; LCDR—light-chain CDR.

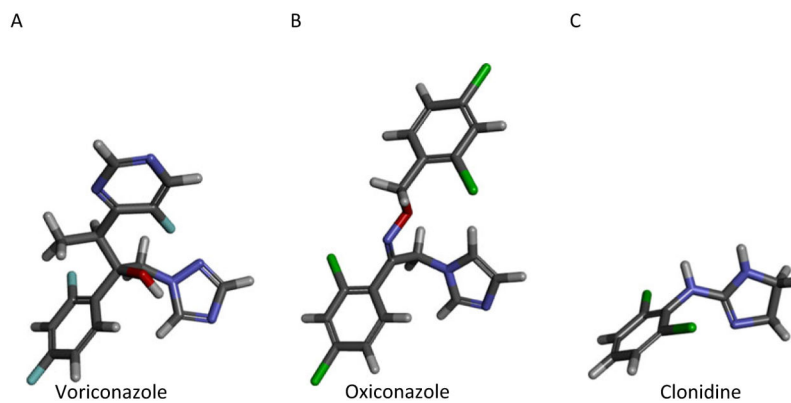


Fig. 3. Voriconazole (A), oxiconazole (B), and clonidine (C), which were identified to inhibit anti-non-Gal IgM xenoantibody, share a limited region of structural similarity suggesting they may inhibit xenoantibody utilizing a common mechanism. Molecules are depicted in three dimensions so as to highlight structural similarities. Gray—Carbon, white—hydrogen, red—oxygen, blue—nitrogen, green—chlorine, teal—fluorine.

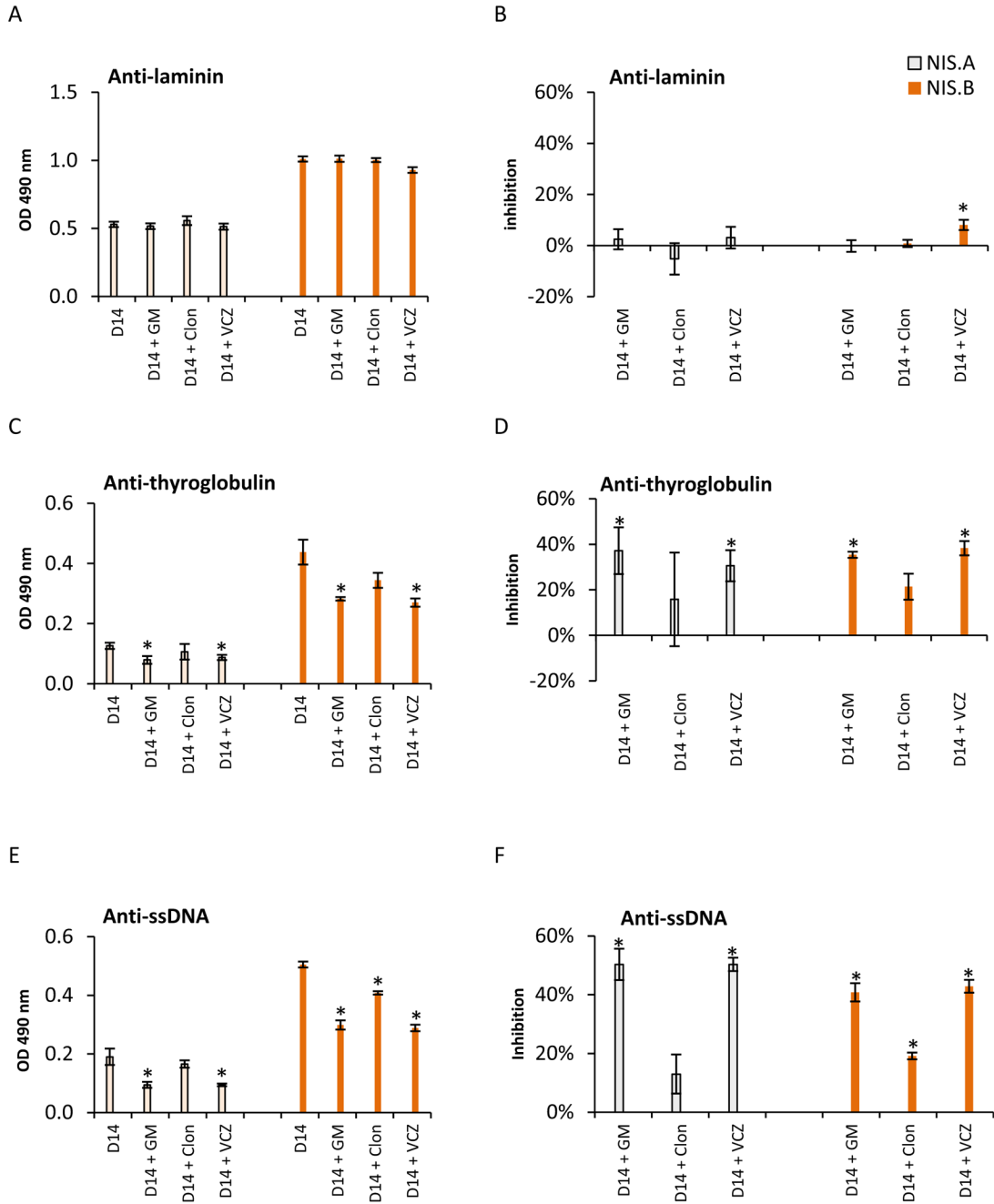


Fig. 4. Clonidine has minimal impact on natural IgM antibodies from non-immunosuppressed rhesus monkeys. Gabexate mesilate (GM), clonidine (Clon), and voriconazole (VCZ) were tested for their ability to inhibit natural antibodies against (A, B) laminin, (C, D) thyroglobulin, and (E, F) single-stranded DNA (ssDNA). These drugs minimally interfere with anti-laminin IgM natural antibodies ($8 \pm 2\%$ inhibition by VCZ). However, both gabexate and voriconazole inhibit natural IgM antibodies against thyroglobulin (16 to 38%) and ssDNA (13 to 50%). In contrast, clonidine only inhibited anti-ssDNA antibodies from

one of the two non-immunosuppressed animals ($19 \pm 1\%$). Values are reported as mean optical density (OD) and % inhibition \pm the standard error of the mean; *Indicates $P < 0.05$ compared to day 14 without drug; non-immunosuppressed animals—NIS.A and NIS.B; % inhibition = $100\% \times [D14_{OD} - (D14 \text{ with drug})_{OD}] / (D14_{OD})$.

Author Manuscript

Author Manuscript

Author Manuscript

Author Manuscript

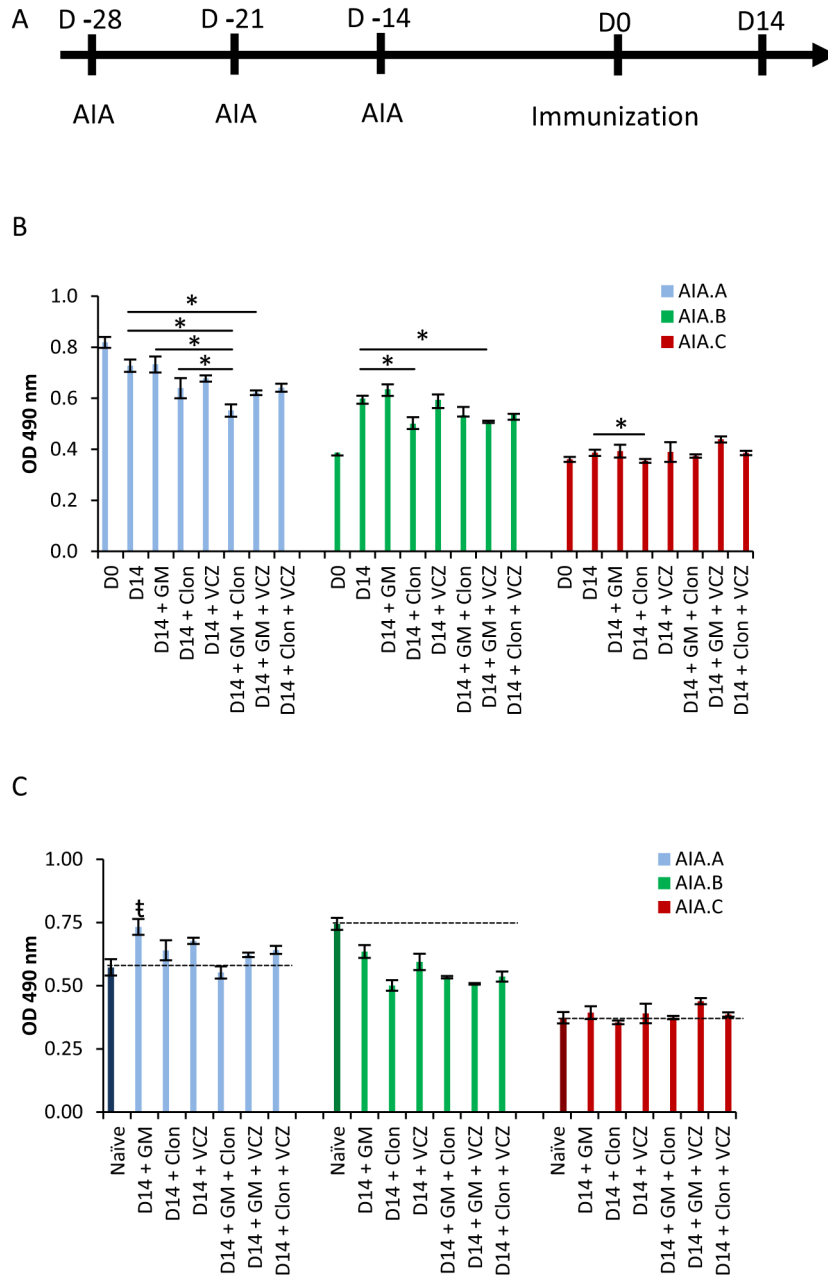


Fig. 5. In all animals tested, clonidine (Clon) is able to inhibit anti-non-Gal IgM detectable by ELISA at day 14 after immunization of anti-idiotypic antibody pre-treated rhesus monkeys (AIA.A, AIA.B, and AIA.C). (A) The in vivo experimental time line. (B) In one animal (AIA.A), the combination of clonidine and gabexate (GM) was significantly more effective than either drug alone. In contrast, the only other effective treatment in this setting was the combination of gabexate and voriconazole (VCZ), which was able to inhibit xenoantibody in two of the three animals tested. (C) After pre-treatment with anti-idiotypic antibody and inhibition of residual xenoantibody, only AIA.A + GM displays significant binding to non-Gal antigen above that of the naïve animal (dashed line/dark bar). Values are reported as

mean optical density (OD) \pm the standard error of the mean; *Indicates $P < 0.05$ compared to day 14 without drug. † indicates $P < 0.05$ that the detectable antibody is above naïve levels.

Author Manuscript

Author Manuscript

Author Manuscript

Author Manuscript

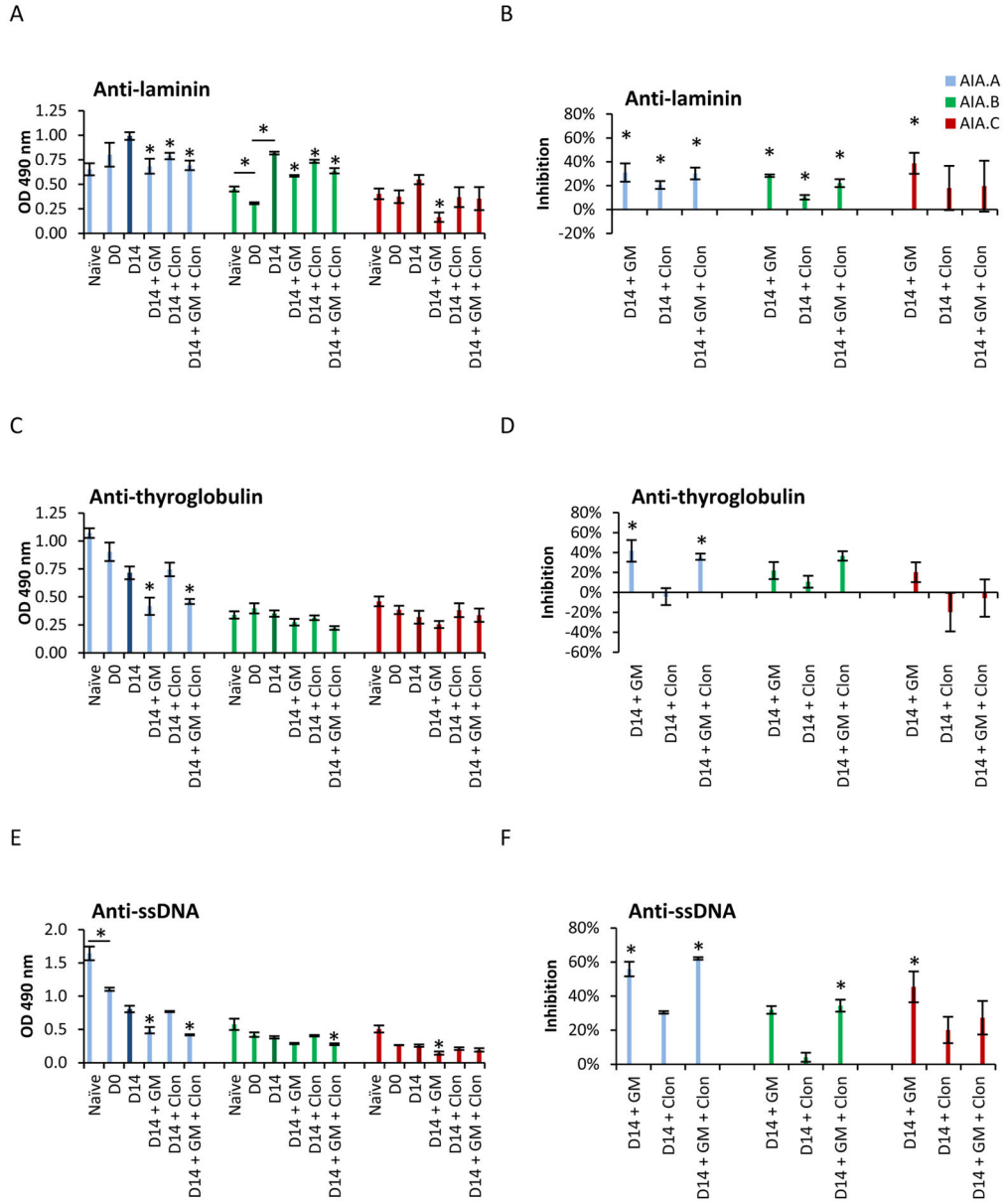


Fig. 6. Clonidine (Clon) has minimal impact on natural IgM antibodies after pre-treatment with anti-idiotypic antibody and immunization with galactosyltransferase knockout (GTKO) pig endothelial cells. (A, B) Clonidine did inhibit some natural antibodies against laminin (10 to 21%). However, clonidine did not interfere with natural IgM antibodies against (C, D) thyroglobulin or (E, F) single-stranded DNA (ssDNA) in this context. In contrast, gabaxate frequently inhibited natural antibodies against laminin (28 to 70%), ssDNA (34 to 56%), and thyroglobulin (42 ± 11%). Values are reported as mean optical density (OD) ± the standard error of the mean; *indicates P < 0.05 compared to day 14 without drug (dark bar) unless otherwise indicated; % inhibition = 100% × [D14_{OD} - (D14 with drug)_{OD}]/(D14_{OD}).

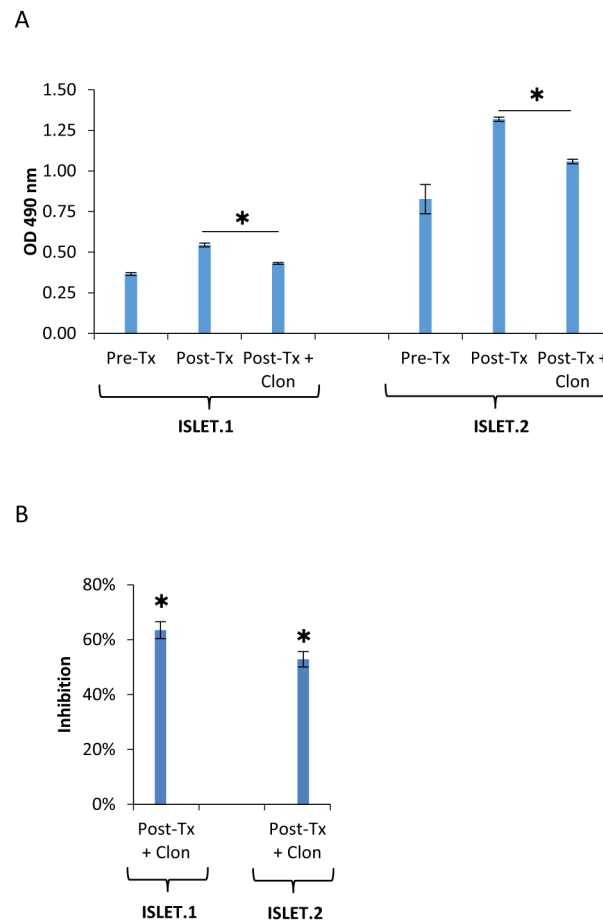
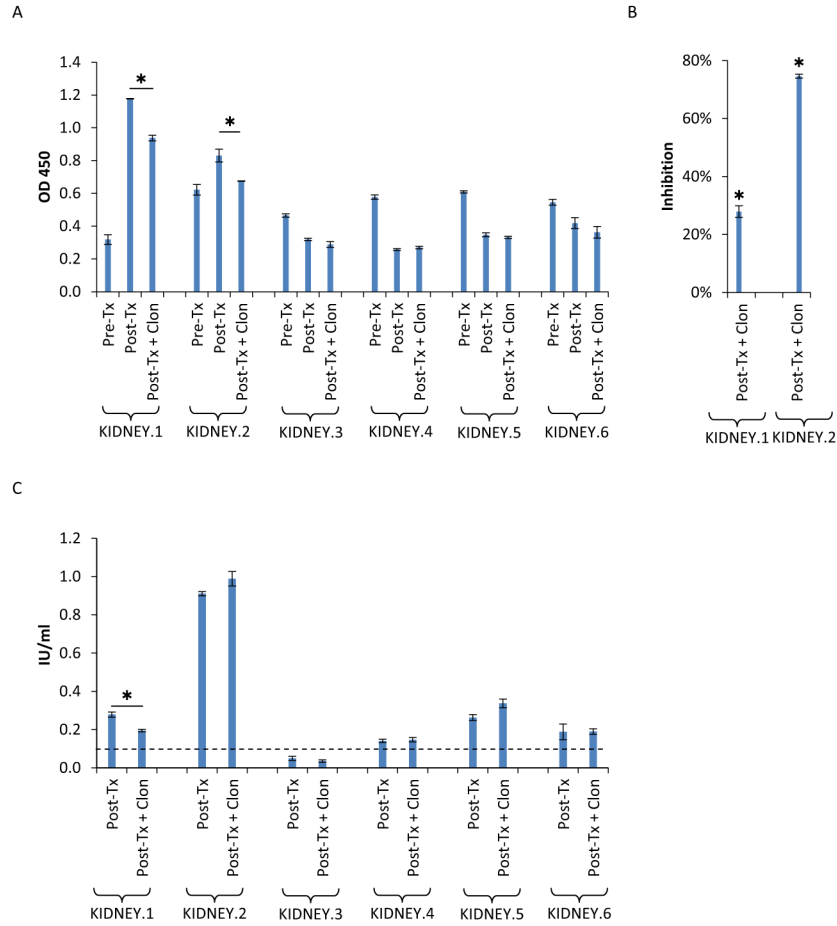


Fig. 7. Clonidine (Clon) is able to inhibit anti-non-Gal IgM elicited in rhesus monkeys (ISELT.1-2) after transplantation with fetal isletlike cell clusters (15×10^6). Although we previously studied the anti-Gal carbohydrate xenoantibody response of these animals [15], they also demonstrated an anti-non-Gal IgM xenoantibody response. Serum used in this study was collected just before transplantation (Pre-Tx) and on postoperative day 8 (Post-Tx). Clonidine was able to inhibit $64 \pm 3\%$ of anti-non-Gal IgM elicited in ISLET.1 and $53 \pm 3\%$ elicited in ISLET.2. Values are reported as mean optical density (OD) \pm the standard error of the mean; *Indicates $P < 0.05$; % inhibition = $100\% \times [D14_{OD} - (D14 \text{ with drug})_{OD}] / (D14_{OD} - D0_{OD})$.

**Fig. 8.**

Clonidine (Clon) is able to selectively inhibit the anti-non-Gal IgM response elicited in baboons in response to galactosyltransferase knockout (GTKO) multitransgenic kidney xenotransplantation. Serum was collected before transplantation (pre-Tx) and at rejection (post-Tx) from six baboons (KIDNEY.1-6). (A, B) Xenografts from two animals (KIDNEY.1-2) were rejected late enough (>100 h) to detect an anti-non-Gal IgM xenoantibody response. Clonidine was able to inhibit $28 \pm 2\%$ of IgM xenoantibody elicited in KIDNEY.1 and $75 \pm 1\%$ elicited in KIDNEY.2. Values are reported as mean optical density (OD) or % inhibition \pm the standard error of the mean; % inhibition = $100\% \times [D14_{OD} - (D14 \text{ with drug})_{OD}] / (D14_{OD} - D0_{OD})$ (C) Clonidine only reduced detectable anti-tetanus toxoid IgG from one of six animals. However, clonidine inhibits anti-non-Gal IgM in all animals, which demonstrated a detectable xenoantibody response suggesting it is highly selective. Anti-tetanus toxoid IgG is known to be protective at 0.1 IU/ml (dashed line). Values are reported as IU/ml \pm the standard error of the mean. *Indicates $P < 0.05$.